Exploring the Binding Mode of Semicarbazide-Sensitive Amine Oxidase/VAP-1: Identification of Novel Substrates with Insulin-like Activity

Luc Marti,[†,‡] Anna Abella,[†,‡] Xavier de la Cruz,[§] Silvia García-Vicente,[†] Mercedes Unzeta,[∥] Christian Carpéné,[⊥] Manuel Palacín,[†] Xavier Testar,[†] Modesto Orozco,[†] and Antonio Zorzano*[,†]

Parc Científic de Barcelona and Departament de Bioquímica i Biologia Molecular, Facultat de Biologia, Universitat de Barcelona, Avda. Diagonal 645, E-08028 Barcelona, Spain, Parc Científic de Barcelona and Institucio Catalana per la Recerca i Estudis Avançats (ICREA), Barcelona, Spain, Departament de Bioquímica i Biología Molecular, Facultat de Medicina, Universitat Autónoma de Barcelona, Barcelona, Spain, and Institut National de la Santé et de la Recherche Médicale (INSERM U 586), IFR 31, CHU Rangueil, 31403 Toulouse Cedex 4, France

Received January 28, 2004

We previously reported that substrates of semicarbazide-sensitive amine oxidase in combination with low concentrations of vanadate exert potent insulin-like effects. Here we performed homology modeling of the catalytic domain of mouse SSAO/VAP-1 and searched through chemical databases to identify novel SSAO substrates. The modeling of the catalytic domain revealed that aromatic residues Tyr384, Phe389, and Tyr394 define a pocket of stable size that may participate in the binding of apolar substrates. We identified a number of amines as substrates of human, rat, and mouse SSAO. The compounds PD0119035, 2,3-dimethoxybenzylamine, and *C*-naphthalen-1-yl-methylamine showed high affinity as substrates of rat SSAO. *C*-Naphthalen-1-yl-methylamine was the only substrate that showed high affinity for human SSAO. *C*-Naphthalen-1-yl-methylamine and 4-aminomethyl-benzenesulfonamide showed the highest capacity to stimulate glucose transport in isolated rat adipocytes. The impact of these findings on the development of new treatments for diabetes is discussed.

Introduction

Semicarbazide-sensitive amine oxidase/vascular adhesion protein-1 (SSAO/VAP-1) is a bifunctional protein with enzymatic and adhesion functions. It has copper-containing amine oxidase activity (EC 1.4.3.6) that converts primary amines to aldehydes, with the concomitant production of hydrogen peroxide and ammonia. SSAO activity is characterized by broad substrate selectivity among species. The enzyme readily oxidizes exogenous (benzylamine, tyramine) or endogenous (phenylethylamine, histamine) aromatic primary amines and also catalyzes the oxidation of endogenous (methylamine, aminoacetone) aliphatic primary amines.[1−5] In addition to its enzymatic function, SSAO/VAP-1 is involved in the interaction between lymphocytes and endothelial cells.[6,7]

SSAO/VAP-1 is highly expressed in adipocytes, where it is localized mainly in plasma membrane in an insulin-independent manner.[8,9] Substrates of this enzyme, such as benzylamine or tyramine, exert a variety of insulin-like effects in human, rat and mouse adipose cells.[8,10−13] In isolated rat adipocytes or in 3T3-L1 adipocytes, the combination of SSAO substrates and low ineffective concentrations of vanadate causes a potent stimulation of glucose transport, GLUT4 recruitment to the cell surface, lipogenesis, and inhibition of lipolysis.[8,10,11,13] The insulin-like effects of the combination of SSAO substrates and vanadate in adipose cells require intact SSAO activity. However, the amine-induced stimulation of glucose transport is abolished by the addition of catalase to the incubation medium and is independent of the generation of the aldehyde derivative.[8,10,11] SSAO substrates also promote adipogenesis in mouse preadipocytes.[14] The incubation of adipocytes in the presence of SSAO substrates and vanadate causes the generation of peroxovanadate compounds, inhibition of protein tyrosine phosphatase, and activation of IRS proteins and phosphatidylinositol 3-kinase activity.[10,15]

The combination of benzylamine and vanadate exerts a very potent anti-diabetic action in diabetic rats. These effects are attributed to the insulin-like effects of SSAO substrates and vanadate on adipose cells. Acute treatment with benzylamine and vanadate enhances muscle glucose transport in nondiabetic rats and glucose tolerance in nondiabetic, in streptozotocin-induced diabetic and in Goto-Kakizaki diabetic rats.[15,16] In addition, chronic treatment with these compounds lowers hyperglycemia, reduces muscle insulin resistance, and enhances glucose disposal in adipose cells.[15,16] Given the insulin-like effects of SSAO substrates in adipose cells and their impact on whole-body glucose homeostasis, it is pertinent to identify the pharmacophoric characteristics that modulate the recognition of substrates by SSAO. This information would be useful for the design of new prodrugs that generate peroxovanadate locally and mimic insulin-like effects in relevant target tissues.

Results

Modeling of the Catalytic Domain of SSAO/VAP-1. The homology modeling protocol led to a model of the

* To whom correspondence should be addressed. Tel: 34-93-4037197. Fax: 34-93-4034717. E-mail: azorzano@pcb.ub.es.

† Parc Científic de Barcelona and Departament de Bioquímica i Biologia Molecular, Facultat de Biologia, Universitat de Barcelona.

‡ Both authors contributed equally to the study.

§ Parc Científic de Barcelona and Institucio Catalana per la Recerca i Estudis Avançats (ICREA).

∥ Departament de Bioquímica i Biología Molecular, Facultat de Medicina, Universitat Autónoma de Barcelona.

⊥ Institut National de la Santé et de la Recherche Médicale (INSERM U 586).

10.1021/jm0499211 CCC: $27.50
Published on Web 08/28/2004

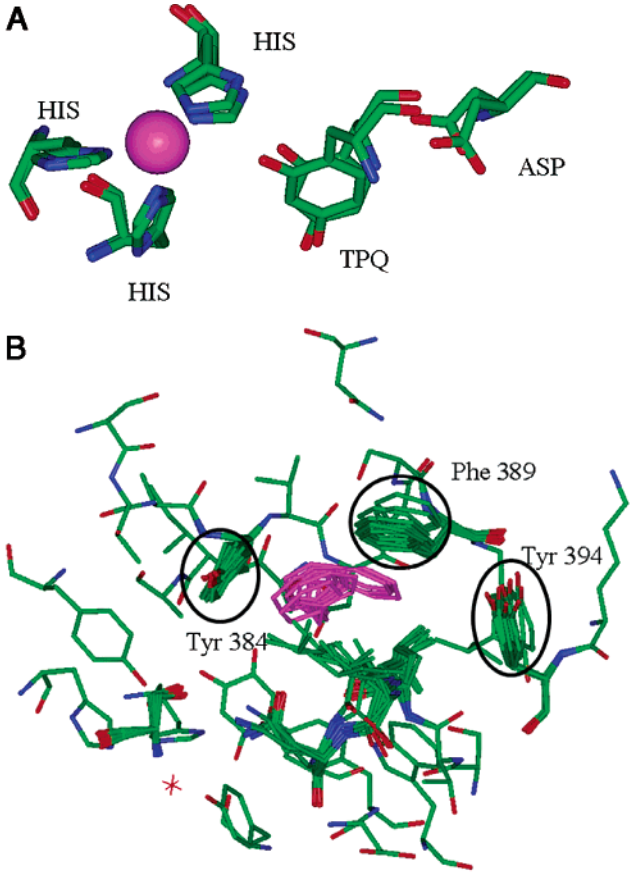

Figure 1. Active centers of SSAO and substrate binding-site residues of SSAO. (A) Superimposed active centers of the *H. polymorpha* and *E. coli* SSAO. Green: carbon atoms. Red: oxygen atoms. Blue: nitrogen atoms. The magenta sphere corresponds to the copper atom. (B) Flexibility of the substrate binding-site residues of mouse SSAO/VAP-1. Ten snapshots, taken every 100 ps, of the molecular dynamics simulation are shown superimposed. The benzylamine molecule is shown in magenta, and the protein atoms are colored following the same scheme as in panel A. Only residues close to the binding site are shown.

SSAO/VAP-1 structure that was validated following standard procedures (see Experimental Section). Validation steps confirmed that the covalent terms have been correctly modeled, and that no important steric contacts were present in the structure. Because the structure of the active site was carefully defined by means of geometrical restraints (see Experimental Section), we expect a better quality in this crucial part of the molecule than in other regions for which no additional information was used.

A restrained molecular dynamics simulation was performed to explore the flexibility of key side chains at the binding site in the presence of benzylamine. This simulation showed (Figure 1B) relatively small fluctuations in the structure of the latter, thus suggesting that the model provides a reasonable definition of the pharmacophore, supporting its use for the design of new putative substrates.

In addition, analysis of the molecular dynamics refined models of the SSAO binding site indicates that the latter is part of a larger pocket, defined by five residues: Tyr384, Phe389, Tyr394, Leu469, and Asn470. Within this cluster, Tyr384, Phe389, and Tyr394 showed well-ordered orientations and defined a stable cavity

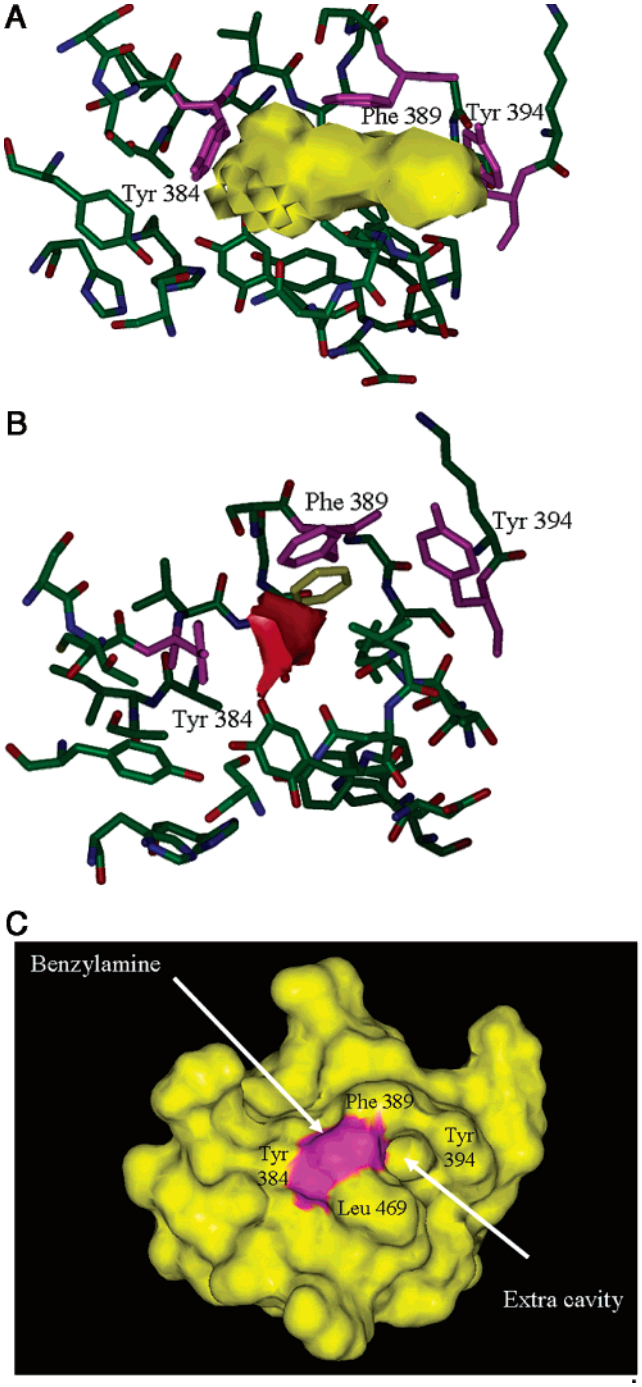

Figure 2. Analysis of the substrate binding site of mouse SSAO/VAP-1. (A) Cavity analysis of the substrate binding site of mouse SSAO/VAP-1. Shown in yellow is the cavity defined at the binding site using the SURFNET program;[17] shown in magenta are residues Tyr384, Phe389, and Tyr394. Only residues close to the binding site are shown. (B) cMIP analysis of the substrate binding site. Shown in red is the potential when using the prototypical O^+ ($q = 0.3e^+$) probe; shown in magenta are residues Tyr384, Phe389, and Tyr394. The same residues as in Figure 1B and panel A are shown, and orientation was slightly changed in order to improve visualization. (C) Molecular surface of the active site of mouse SSAO bound to benzylamine (in magenta). The extra hydrophobic cavity close to the aromatic ring of benzylamine is marked with an arrow.

with an overall rectangular shape, as shown by cavity calculations done with Laskowsky's program[17] (see Figure 2A). Interestingly, when electrostatic effects were taken into account by using classical molecular interac-

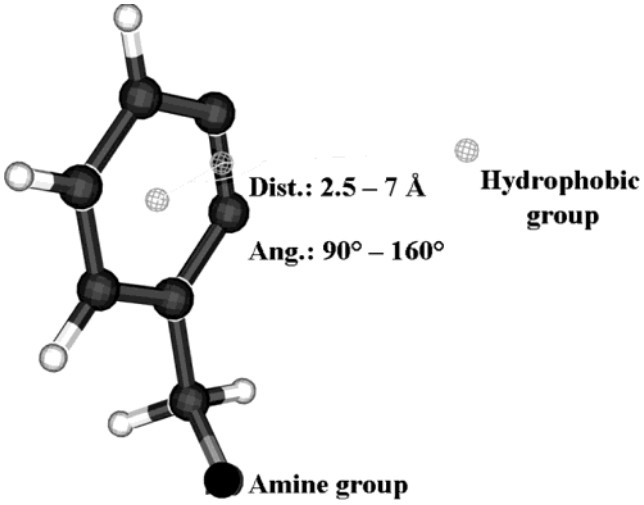

Figure 3. Pseudomolecule (pharmacophore) used to scan the small-molecule 3-D databases.

tion potentials[18] (cMIP; see Figure 2B), a clear binding site was observed for positive charges located at the expected binding site for the amine group of the substrate.

The binding of benzylamine at the active site results in a decrease in the average accessible surface area (ASA) of residues Tyr384, Phe389, Leu469, and Asn470: 21.0 (7.2), 32.8 (3.7), 26.2 (18.3), and 23.6 (25.1) Å^2, respectively (standard deviations computed for the snapshots shown in Figure 1B). This confirms that the latter are in close contact with benzylamine and become largely buried upon its binding. However, Tyr394 did not show any significant change in ASA, remaining quite accessible after binding of benzylamine, leaving a small cavity, located between the benzylamine aromatic ring and the phenol ring of Tyr394 (Figures 1B and 2C). This cavity was also limited by the side chains of Phe389 and Leu469 and, accordingly, showed a marked hydrophobic character. We hypothesized a priori that filling this cavity with apolar groups would lead to compounds with an enhanced binding ability to mouse SSAO. However, for our purposes, this cavity was used as a test for the goodness of the model. That is, if the proposed binding mode is correct, the replacement of the benzylamine benzene ring by a larger aromatic group would not impede binding of the drug. On the contrary, if the binding mode is incorrect, the binding of larger aromatic groups will not be tolerated because of steric constraints in the relatively narrow active site (Figure 1B and Figure 2).

Identification of Novel SSAO Substrates. To identify putative substrates of SSAO, from the above binding model we defined a pseudomolecule (defining the pharmacophore; see Figure 3), which was then used to screen 3-D databases of small molecules (BioByte, Maybridge, Derwent, NCI). Note that at this stage our objective was not to identify more efficient new substrates, but rather to determine the capacity of the proposed model to predict the binding capacity of new molecules. That is, the usefulness of the pharmacophore hypothesis in recovering active molecules would increase our confidence in the proposed binding mode.

The pseudomolecule proposed was designed to fill the benzylamine binding pocket with molecules having a methylamine attached to an aromatic group. This pocket was defined by Tyr384, Phe389, Tyr394, Leu469, and Asn470. However, at this stage our efforts focused on the region around Tyr384, Tyr394, and Phe389, since these residues showed the most stable orientations during the dynamics. Benzylamine was used as core, and the database was searched for aromatic groups able to fill the small cavity that remained after benzylamine binding. The location of the hydrophobic group (Figure 3) was defined relative to the benzylamine aromatic ring. Given the roughness of our structural model, we kept the location of the hydrophobic group within broad limits.

After exploring several databases, namely, BioByte (BioByte Corporation, Claremont, CA), Maybridge (Maybridge, Cornwall, U.K.), Derwent (Derwent World Drug Index Ver., Philadelphia, PA), and NCI,[19] we recovered the distinct hits using the CATALYST program, from Accelrys Inc. All were then fitted into the binding site using the cMIP program[18] and refined manually. Molecules with bad interactions, and others that did not fulfill the conditions to be substrates, were omitted from the study. Finally, a reduced set of 5 molecules were studied experimentally to check for new substrates, and to verify the goodness of the binding mode proposed. In parallel, we also analyzed the activity of another series of amines, which could be a priori substrates of SSAO. These include amikacin, bekanamycin, BN 50125, BN 50192, butirosin, capreomycin, ceforanide, dibekacin, lividomycin A, lysine, *N*-acetyl muramic acid, neamine, neomycin, netilmycin, paramonycin, PD0111700, pyridoxamine, polylysine, ribostamycin, sisomycin, tobramycin, xylostatin, 2-aminomethyl-6-methoxy-phenol, and 1-aminomethylnaphthalen-2-ol. If the pharmacophore model is useful, the small set of compounds selected by the pharmacophoric restraints should be much more enriched in active compounds than the second set, which was selected without considering structural information.

Two types of screening tests were performed; the first was based on the capacity of putative substrates (at concentrations of 0.1 and 1 mM) to inhibit SSAO activity in human or rat adipose tissue membranes (assayed as benzylamine oxidation). Putative SSAO substrates were selected as compounds with a primary amine and with no substituents on the β-carbon.[2] Putative substrates with an IC_{50} lower than 1 mM were selected for further analysis. The second screening involved the detection of hydrogen peroxide production in the presence of 0.1 or 1 mM compound and 50 μg or 10 μg of membrane proteins obtained from rat or human adipose tissue, respectively. The five molecules selected using the pharmacophore hypothesis, 4-aminomethyl-benzenesulfonamide (ABS), 2,3-dimethoxy-benzylamine (DMB), *C*-naphthalen-1-yl-methylamine (NM), PD0119035, and PD0125999, were active and strongly inhibited benzylamine oxidation in membrane preparations from the two tissues. These compounds showed a substantial capacity to produce hydrogen peroxide by catalysis of rat SSAO from adipose tissue membranes (Figure 4A). In addition, they acted as substrates of human SSAO (Figure 4B), and this enzyme showed a higher capacity to metabolize all these compounds than rat SSAO (Figure 4). None of the molecules of the second set

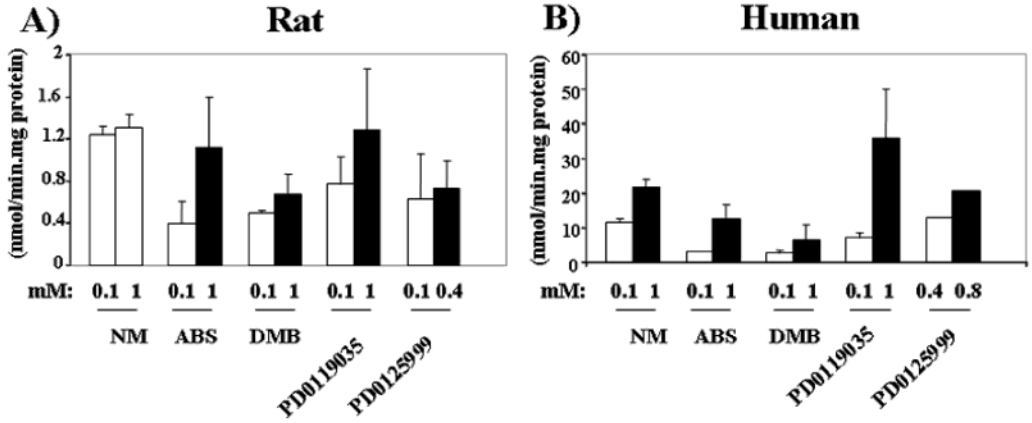

Figure 4. SSAO-dependent oxidation of several compounds. SSAO-dependent oxidation of distinct compounds assayed at 0.1 and 1 mM in rat or human adipose tissue membranes with the exception of compound PD0125999, which was assayed at 0.1 and 0.4 mM in rat SSAO and 0.4 and 0.8 in human SSAO. Crude membranes (around 50 μg protein/assay) were incubated for 30 min at 37 °C in the presence of the concentrations of compounds indicated. Hydrogen peroxide formation caused by SSAO activity was measured spectrophotometrically. Rates of benzylamine oxidation at 0.1 or 1 mM concentrations were 2.1 ± 0.2 and 1.9 ± 0.1 nmol per min per mg of protein, respectively, in rat SSAO and 149 ± 48 and 459 ± 23 nmol per min per mg of protein in human SSAO. Data represent the means ±SEM from five to seven experiments.

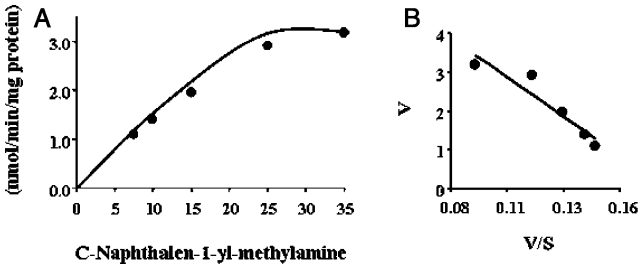

Figure 5. Concentration dependence of *C*-naphthalen-1-yl-methylamine as a substrate of rat SSAO. Crude membranes from rat adipose tissue (around 50 μg protein/assay) were incubated for 30 min at 37 °C in the presence of a range of *C*-naphthalen-1-yl-methylamine concentrations (μM). Hydrogen peroxide formation caused by SSAO activity was measured spectrophotometrically. Panels show a representative experiment (panel B is an Eadie−Hoffstee plot) performed in triplicate.

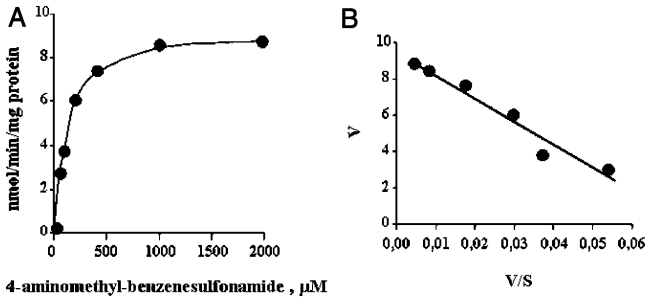

Figure 6. Concentration dependence of 4-aminomethyl-benzenesulfonamide as a substrate of rat SSAO. Crude membranes from rat adipose tissue (around 50 μg protein/assay) were incubated for 30 min at 37 °C in the presence of a range of 4-aminomethyl-benzenesulfonamide concentrations (μM). Hydrogen peroxide formation caused by SSAO activity was measured spectrophotometrically. Panels show a representative experiment (panel B is an Eadie−Hoffstee plot) performed in triplicate.

(which contained 25 compounds) showed any activity. Therefore, these results confirm/demonstrate the usefulness of the refined 3-D binding mode and the pharmacophore defined from it.

Enzymatic analysis of rat SSAO indicated that compounds such as NM or ABS fitted Michaelis−Menten kinetics (Figures 5 and 6). Low and similar K_m values were obtained for benzylamine, NM, DMB, and PD0119035 for rat SSAO; K_m values were high for ABS and PD0125999 (Table 2). Maximal rates of rat SSAO catalysis were obtained for benzylamine and NM (Table 2), lower values being found for the other substrates. In parallel, the enzymatic efficacy of rat SSAO was similar for benzylamine and NM (Table 2). When assayed in mouse SSAO obtained from adipose tissue, NM showed high affinity (K_m values were lower than for benzylamine). In contrast, DMB was a low affinity substrate (Table 2) and, similarly, to the rat enzyme, mouse SSAO showed a similar enzymatic efficacy for benzylamine and NM.

In human SSAO, kinetic analysis indicated that NM had a lower K_m than benzylamine (Table 2) while the other substrates showed higher values (Table 2). Under these conditions, V_{max} values for benzylamine were higher than those of the novel SSAO substrates (Table 2). This finding indicates some structural differences between mouse, rat, and human SSAO, which are reflected in changes in the catalytic profile of the enzyme in response to diverse substrates.

Table 1. Distance and Torsional Angle Restraints for the Active Site Residues[a]

TPQ471 O2−Cu	4.48 Å
TPQ471 O4−Cu	6.12 Å
HIS520 $N_{\epsilon 2}$−Cu	2.23 Å
HIS522 $N_{\epsilon 2}$−Cu	2.03 Å
HIS684 $N_{\delta 1}$−Cu	2.15 Å
ASP386 χ_1	105.03°
TPQ471 χ_1	0.82°
HIS520 χ_1	286.76°
HIS522 χ_1	263.34°
HIS684 χ_1	183.43°

[a] $\chi 1$ is the first side chain torsion angle; the sequence numbering corresponds to the structural model of mouse SSAO (AOC3).

Activation of Glucose Transport in Isolated Rat Adipocytes. The incubation of isolated rat adipocytes in the presence of SSAO substrates, such as benzylamine and vanadate, stimulates glucose transport.[8] Thus, here we analyzed whether the novel SSAO substrates exerted the same effect. Incubation of adipose

Table 2. Kinetic Properties of Novel SSAO Substrates Assayed in the Presence of Human, Rat, or Mouse SSAO[a]

	K_m (μM)	V_{max} (nmol/min/mg protein)	V_{max}/K_m
(A) Rat SSAO			
benzylamine	6.7 ± 0.6	2.6 ± 0.1	0.39
C-naphthalen-1-yl-methylamine	10.2 ± 2.0	2.9 ± 0.3	0.28
4-aminomethyl-benzenesulfonamide	100 ± 22	0.7 ± 0.3	0.007
2,3-dimethoxy-benzylamine	16.8 ± 4.0	1.1 ± 0.1	0.06
PD0119035	14.2 ± 11.4	0.7 ± 0.2	0.05
PD0125999	157	0.7	0.004
(B) Mouse SSAO			
benzylamine	33 ± 5	9.7 ± 3.9	0.29
C-naphthalen-1-yl-methylamine	4.8 ± 3.1	3.2 ± 1.2	0.66
4-aminomethyl-benzenesulfonamide	nd[b]	nd	nd
2,3-dimethoxy-benzylamine	294	3.2	0.01
PD0119035	nd	nd	nd
PD0125999	nd	nd	nd
(C) Human SSAO			
benzylamine	175 ± 18	456 ± 19	2.61
C-naphthalen-1-yl-methylamine	72 ± 34	36 ± 13	0.50
4-aminomethyl-benzenesulfonamide	4886 ± 378	61 ± 25	0.01
2,3-dimethoxy-benzylamine	nd	nd	nd
PD0119035	983 ± 378	117 ± 47	0.12
PD0125999	2314	114	0.05

[a] Crude membranes (around 50 μg of protein/assay) obtained from human, rat, or mouse adipose tissue were incubated for 30 min at 37 °C in the presence of a range of compound concentrations. Hydrogen peroxide formation caused by SSAO activity was measured spectrophotometrically. Kinetic parameters were obtained through Eadie−Hoffstee plots. Data represent the means ± SEM from three to four separate experiments. [b] Not determined.

cells in the presence of both benzylamine and vanadate greatly enhanced glucose transport (near 80% of maximal insulin action) in isolated rat adipocytes (Figure 7A). Under these conditions, incubation in the presence of NM and vanadate also markedly stimulated this transport in a concentration-dependent and SSAO-dependent manner (Figure 7A). The maximal effect in the presence of 0.1 mM NM and 0.1 mM vanadate was comparable to that observed for benzylamine/vanadate (70% of maximal insulin-stimulated glucose transport) (Figure 7A). The stimulatory effect of NM/vanadate was blocked in the presence of semicarbazide and was insensitive to pargyline, a MAO inhibitor (Figure 7A). NM did not stimulate glucose transport in the absence of vanadate (data not shown).

The substrate ABS also greatly enhanced glucose transport in isolated rat adipocytes (60% of benzylamine effects), but maximal stimulation was observed only at high concentrations (Figure 7B). The effects of ABS/vanadate on glucose transport were also blocked by semicarbazide (Figure 7B). The compounds DMB, PD0119035, and PD0125999 caused a modest increase in glucose transport in the presence of vanadate (ranging from 5% to 10% of maximal effect of benzylamine/vanadate) (Figure 7C).

Discussion

In this article we study the binding site of the enzyme SSAO using homology modeling, together with molecular dynamics simulations. We find that it is is well defined and stable, with a high capacity to interact with the cationic amino group of benzylamine and related molecules. Furthermore, a cluster of three aromatic residues which contact the substrate in the channel, Tyr384, Phe389, and Tyr394 in mouse SSAO define a conserved hydrophobic pocket which stabilizes the binding of aliphatic or aromatic substrates. The presence of this pocket explains why aromatic amines with a more extended aromatic core are recognized by SSAO as substrates, thus supporting our model of the binding site.

SSAO recognizes aliphatic and aromatic amines. Aliphatic amines that are SSAO substrates include compounds such as methylamine, aminoacetone, ethylamine, propylamine, butylamine, pentylamine, hexylamine, heptylamine, octylamine, nonylamine, and decylamine.[20−22] Aromatic compounds that are substrates of SSAO include biogenic amines such as benzylamine, tyramine, 2-phenylethylamine, histamine, dopamine, and tryptamine.[5] In this study, molecular modeling has allowed the identification of novel substrates of SSAO that include ABS, DMB, NM, and the aminomethylpyrrolidine derivatives PD0125999 and PD0119035. Thus, our study shows that other benzylamine derivatives may be efficient SSAO substrates, and that other families of compounds derived from *C*-naphthalen-1-yl-methylamine or aminomethylpyrrolidine are also SSAO substrates. In this regard, it is pertinent to mention that human, rat, and mouse SSAO show a similar enzymatic efficacy for benzylamine and *C*-naphthalen-1-yl-methylamine (NM).

The compounds identified as substrates showed marked differences in their comparative affinities to SSAO, which also varied in distinct species. Thus, in rat SSAO, K_m values were low and similar for benzylamine, NM, DMB, and PD0119035. When assayed in mouse SSAO from adipose tissue, NM also showed high affinity (K_m values were even lower than for benzylamine) whereas DMB was a low affinity substrate. In human SSAO, kinetic analysis indicated that NM had a lower K_m than benzylamine whereas the other substrates showed very high values. Maximal rates of rat SSAO catalysis were obtained for benzylamine and NM, whereas values were low for the other substrates. In mouse and human SSAO, V_{max} values were maximal for benzylamine compared with the novel SSAO substrates. Human SSAO showed K_m values for all substrates analyzed that were higher than in rat and in mouse adipose tissue. Data regarding K_m values for benzylamine are consistent with previous observations.[22,23] Clearly, small structural differences between mouse, rat, and human are responsible for the distinct enzymatic properties of the three enzymes. However, sequence alignments and 3-D models indicate a common binding mechanism for the SSAO of distinct origin studied here, which is confirmed by our experimental results. More experimental data on affinity differences between the human and mouse enzymes could be used to improve our 3-D model of the active site of SSAO.

The identification of the pharmacophore requirements of SSAO substrates and the discovery of a novel series of substrates for this enzyme, which include two previously unrecognized families of compounds, are highly

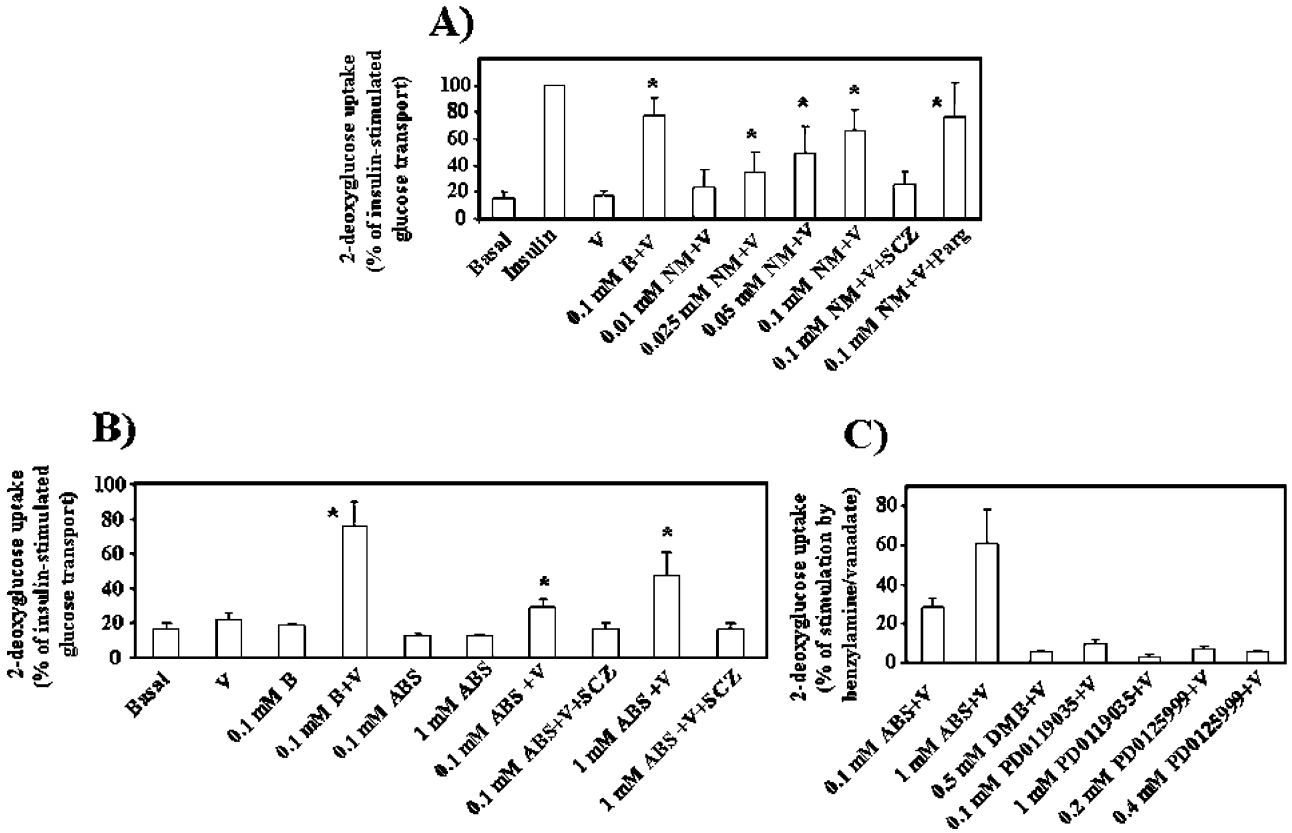

Figure 7. Stimulation of glucose transport in isolated rat adipocytes. Rat adipocytes were incubated for 45 min in incubation medium without (basal) or with 100 nM insulin, varying millimolar concentrations of amines (B, benzylamine; NM, *C*-naphthalen-1-yl-methylamine; ABS, 4-aminomethyl-benzenesulfonamide; DMB, 2,3-dimethoxy-benzylamine; PD0119035 and PD0125999), 0.1 mM sodium orthovanadate (V), 1 mM semicarbazide (SCZ) or 1 mM pargyline (Parg). Subsequently, 2-deoxyglucose uptake was measured over a 10-min period. Results are mean ± SE of four to six experiments. Asterisks (*) indicates statistically significant difference with basal rates of glucose transport, at $P < 0.05$. Rates of glucose transport in panel C were statistically significant different from basal levels with all compounds studied, at $P < 0.05$.

relevant. First, our data enlarges the number of xenobiotic amines that may be metabolized by SSAO in vivo. A second consideration is that some of these compounds can be used pharmacologically to regulate glucose homeostasis. In this regard, we found that, in combination with low concentrations of vanadate, all the novel SSAO compounds stimulated glucose transport in adipose cells. Thus, NM and vanadate markedly enhanced glucose transport in a concentration-dependent manner and the maximal effect of NM/vanadate was comparable to the effect of benzylamine/vanadate (70% of maximal insulin-stimulated glucose transport). ABS also caused a large improvement in glucose transport in isolated rat adipocytes (60% of benzylamine effects). In addition, the stimulatory effects of NM/vanadate or ABS/vanadate were blocked in the presence of semicarbazide and were insensitive to MAO inhibition. These data are in agreement with previous observations that indicate that the combination of SSAO substrates, such as benzylamine or tyramine, and vanadate stimulates glucose transport and GLUT4 recruitment to the cell surface in isolated rat adipocytes.[8,10,11]

Interestingly, our data show that the maximal stimulatory effects of NM and ABS in combination with vanadate on glucose transport by isolated rat adipocytes were fairly similar in spite of major differences in the affinity of these substrates to rat adipose SSAO. A corollary of these data is that affinity of the substrates to SSAO (K_m values) is not a good predictor of their capacity to enhance glucose transport. Instead, the maximal catalytic activity (V_{max}) parameter is a better indicator of the capacity of SSAO substrates to activate adipose glucose transport. This finding is of special interest for the activation of this transport in human adipose cells, whose SSAO is characterized by low affinity toward substrates.

Experimental Section

Materials. 2-[1, 2-^{3}H]-D-Deoxyglucose (26 Ci/mmol) was purchased from NEN Life Science Products, and [^{14}C]benzylamine (59 Ci/mmol) was from Amersham Pharmacia Biotech. Purified porcine insulin was a kind gift from Eli Lilly (Indianapolis, IN). Streptozotocin, semicarbazide hydrochloride, benzylamine hydrochloride, sodium orthovanadate, *C*-naphthalen-1-yl-methylamine, 2,3-dimethoxy-benzylamine, 4-aminomethyl-benzenesulfonamide, and other chemicals were purchased from Sigma Aldrich (St. Louis, MO). Collagenase type I was obtained from Worthington. PD0119035 and PD0125999 were from Parke-Davies.

Adipocyte Membrane Preparations. Isolated fat cells from human donors, rats, or mice were disrupted for total membrane preparation by hypo-osmotic lysis in a 20 mM HES buffer and an antiprotease cocktail as reported.[8] Protein concentrations were determined by the Bradford method[24] with γ-globulin as a standard.

Amine Oxidase Activity Assays. The radiochemical determination of semicarbazide-sensitive amine oxidase activity was performed as described by Fowler and Tipton,[25] with slight modifications.[11] The reaction was performed in 200 μL of 50 mM phosphate buffer at 37 °C in the presence of radioactive benzylamine (100 μM; 50 mCi/mmol) at pH 7.4 for 30 min.

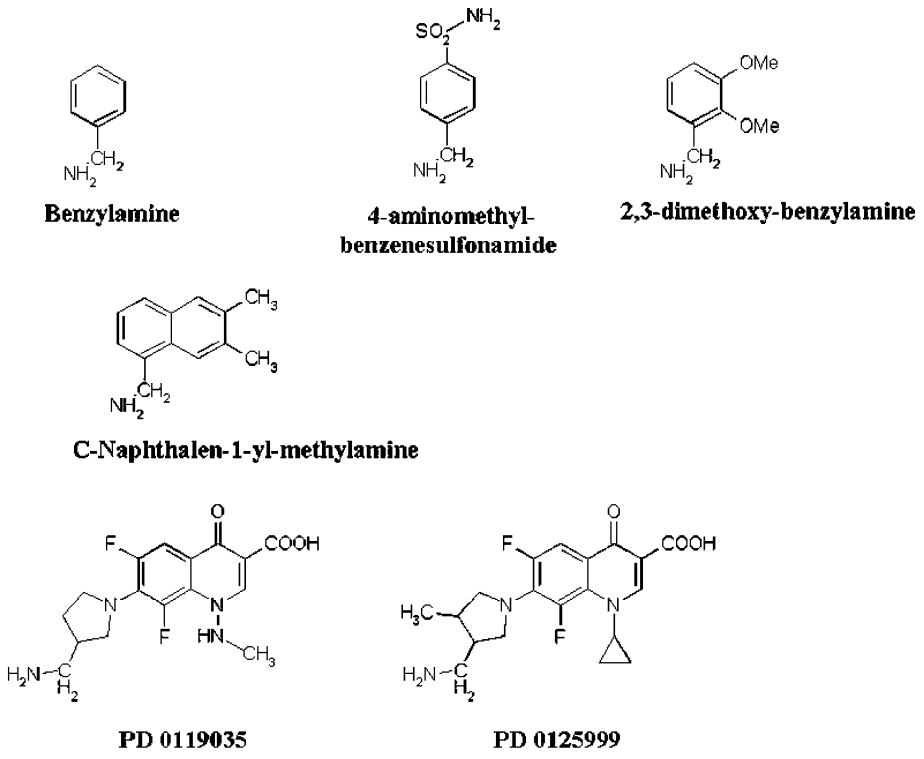

Figure 8. SSAO substrates.

Reactions were arrested by addition of 50 μL of 4 N HCl, and the products were extracted into toluene/ethyl acetate 1:1 (v/v) before liquid scintillation counting. Blank values were measured in assays preincubated for 15 min in the presence of 1 mM semicarbazide to totally inhibit SSAO activity. To examine the capacity of unlabeled amines to interfere with the metabolism of benzylamine by SSAO, competition studies were performed by preincubating the membrane preparations with the distinct amines at the concentrations indicated for 15 min before the addition of the radiolabeled benzylamine.

The continuous spectrophotometric detection of SSAO-dependent H_2O_2 production was performed following the procedure described by Holt et al.,[26] based on a peroxidase-coupled reaction. Rat or human adipocyte membranes and horseradish peroxidase were incubated in the presence of homovanillic acid and aminoantipirine, and the amine was tested. The change in absorbance at 498 nm was followed over time. Time course assays were performed to ensure that initial rates of the reaction were measured with precision. Inhibition of MAO activity in human membrane preparations was done by preincubating the membranes for 15 min with 10 μM pargyline. Protein concentrations were determined by the Bradford method[23] with γ-globulin as a standard.

Glucose Transport Measurements in Isolated Rat Adipocytes. Adipocytes were isolated from epididymal fat pads of healthy male Wistar rats (180−220 g), as reported.[8,11] After a preincubation period of 45 min at 37 °C, each vial, which contained 400 μL of cell suspension in KRBHA and the drugs being tested, received an isotopic dilution of 2-deoxy-D-[^{3}H]glucose (2-DG), giving a final concentration of 0.1 mM, equivalent to approximately 1300000 dpm/vial. 2-DG transport assays were performed as reported.[8,11]

Theoretical Calculations. The structure of mouse SSAO was modeled using the standard software package MODELLER.[27] The resulting model was used to define the pharmacophore by combining both restrained molecular dynamics simulations and structural analysis tools. The main steps of the modeling protocol followed were(a) selection of the templates, (b) definition of the domain boundaries for the templates and the target sequence, (c) alignment of the templates and the target sequence, and (d) model generation and refinement.

Selection of the Templates. One of the main objectives of the homology modeling procedure was to generate a good model of the active site of mouse SSAO (AOC3).[7] This would help defining a reasonable pharmacophore to be used in the screening of small-molecule 3-D databases. This was the main criterion used to select the templates for the modeling.

The active center of SSAO is formed by a copper coordination complex which involves 3 histidine residues, a topaquinone (TPQ) residue, and an aspartic residue.[28] This TPQ group, which is crucial for the activity of the enzyme, can show distinct alignments at the active site, and only a few of these are compatible with catalysis. After analysis of the PDB, we selected two structures, 1a2v from *Hansenula polymorpha*[28] and 1spu from *Escherichia coli*,[29,30] as templates for the model because in these two structures the TPQ is in a good orientation for catalysis. The sequence identity between the mouse SSAO and the templates was 31.0% and 32.1%, respectively. Interestingly, superimposition of active site residues for 1a2v and 1spu (Figure 1A) showed good root-mean-square deviations for the atom positions (0.45 Å and 0.72 Å, when excluding and including the critical aspartate residue, respectively).

Definition of the Domain Boundaries for the Templates and the Target Sequence. The domain boundaries of the catalytic subunit of SSAO were taken from the SCOP[31] database: residues 237−656 for 1a2v, and residues 301−721 for 1spu. To derive the N-terminal boundary of the catalytic domain of the target sequence, we used the Pfam[32] SSAO family, removing all the sequences except those of the target protein (mouse AOC3), and the two templates (1a2v and 1spu).

Alignment of the Templates and the Target Sequence. Part of the MODELLER input requires a multiple alignment that includes the templates and the sequence of the target protein (mouse AOC3). To attain this alignment, a conservative two step protocol was followed and we obtained (i) a structure-based alignment for the templates and (ii) a sequence alignment between the templates and the target sequence.

The structural alignment between 1a2v and 1spu was taken from the HOMSTRAD[33] database. The root-mean-square between the two structures was 1.70 Å, when using the Ca atoms for the superimposition. The alignment between the target sequence and the templates was then obtained using

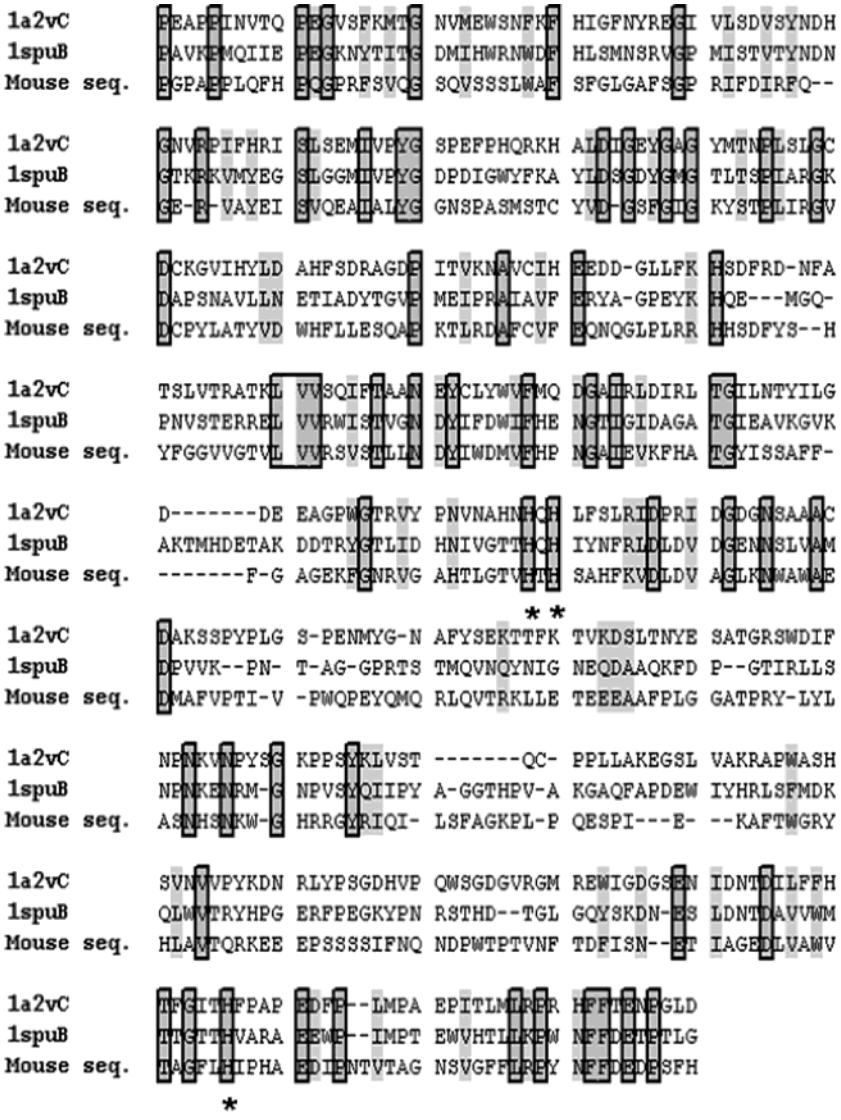

Figure 9. Multiple sequence alignment between SSAO and the two templates used for the modeling (see Experimental Section). Enclosed in boxes are the residues that were identical in the three sequences. The three relevant histidines are labeled with asterisks. Highlighted in gray are similar residues, that is, those with close physicochemical properties.

the CLUSTALW[34] program and the Pfam[32] alignment for the SSAO family. For this purpose, we first edited the Pfam alignment by removing the 1a2v and 1spu sequences.We next aligned the structural (HOMSTRAD) alignment of 1a2v and 1spu with the modified Pfam alignment. Finally, we eliminated all the sequences except those from the target protein and the two templates (1a2v and 1spu), and the resulting alignment (Figure 9) was then used as input for MODELLER.

Model Generation and Refinement. To ensure the quality of the active site model, standard restraints in MODELLER[27] were increased by specific restraints to enforce and preserve the geometry of the active site residues (Table 1). Side chains were automatically placed by MODELLER,[27] following a protocol that uses probability density functions obtained from a database of structural alignments,[27] taking into account distinct types of information, from side chain dihedral angles of the equivalent residue in the templates to the residue environment. The final homology model was then obtained following the standard procedure in MODELLER and tested by means of PROCHECK.[26] An additional control was provided by the PROSA[35] program, which identifies potential problems in protein models. PROSA labels incorrectly modeled residues with positive "energy" values. In our case, this program did not detect any errors in the model except two positive energy peaks. The latter correspond to residues in contact with the second monomer of the biological subunit, which is missing in the model. This results in a poor environment for these residues, leading to positive values of the PROSA-like energy functions,[36] thus explaining the observed values.

The structural properties of the substrate binding site (those residues contacting the substrate, but not involved in its catalysis) were then studied by means of restrained molecular dynamics simulations in the presence of benzylamine, a well-known substrate of the enzyme. To this end, we used the AMBER[37] program to generate a 1 ns molecular dynamics trajectory for the protein−benzylamine complex. The simulation was done at a constant temperature ($T = 300$ K), placing a spherical drop of water of 18 Å radius centered on the C_{d2} carbon of the TPQ residue, which covers the entire active site. Only residues in contact with the substrate, Tyr384, Phe389, Tyr394, Leu468, Leu469, Asn470, and Ser496, were allowed to move during the dynamics, thus allowing the relaxation of their positions. It is important to note that we used this restrained MD protocol to preserve the key pharmacophoric properties of the enzyme, thereby avoiding the drift of the structures away from the original homology model.

Validation of the Model. To validate the model, we chose three molecules from the list of known SSAO substrates, butylamine, dopamine, and tryptamine, and docked them into the model's binding cavity. For this purpose, we used DOCK[38] and cMIP[18] programs. In all three substrates, the best hits

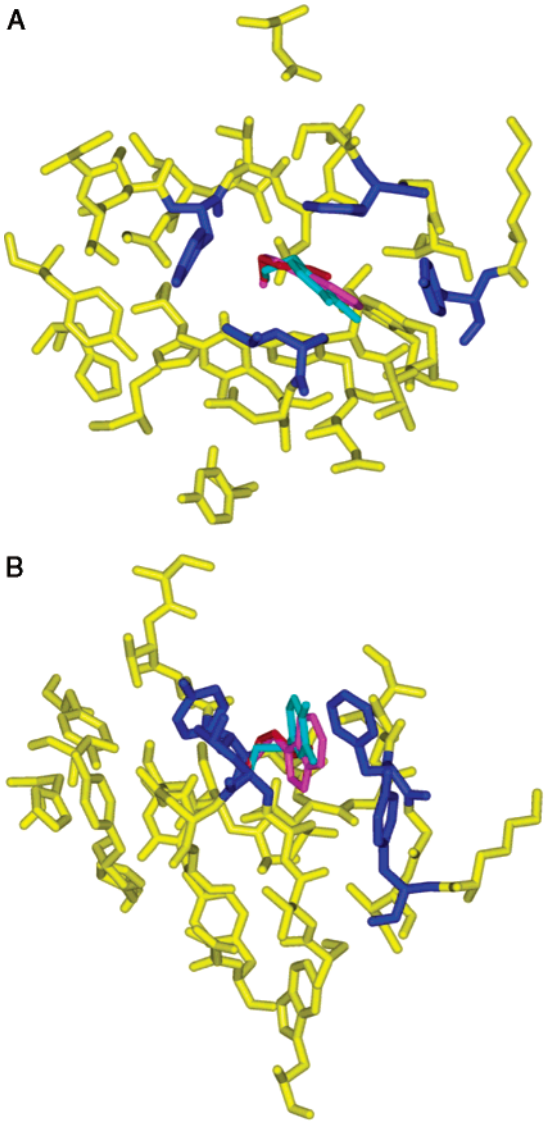

Figure 10. Docking of three known substrates to the binding pocket of the SSAO model (see Experimental Section): butylamine (red), dopamine (light blue), and tryptamine (magenta). Views A and B correspond to upper and lateral views of the binding site with the ligands bound.

were consistent with a productive binding mode, like that shown in Figure 10.

Acknowledgment. We thank Tanya Yates for correcting the English manuscript. This study was supported by research grants from the Dirección General de Investigación Científica y Técnica (PM98/0197, PM99-0046, BIO2003-06848, and BIO2003-09327), Ministerio de Ciencia y Tecnología (SAF2002-02125), Grant SGR01-118 from the Generalitat de Catalunya, European Commission (Quality of Life, QLG-CT-1999-00295), "Accords INSERM/CSIC", "Actions Integrées Franco-Espagnoles PICASSO", COST B17 Action, Fundació Marató de TV3 (300720), and the Instituto de Salud Carlos III RCMN (C03/08), RGDM (G03/212), and RGTO (G03/028). We also thank the Centre de Supercomputació de Catalunya for computational support. A.A. was a recipient of a predoctoral fellowship from the Universitat de Barcelona. L.M. was a recipient of a Marie Curie postdoctoral fellowship from the European Union

Appendix

Abbreviations. SSAO, semicarbazide-sensitive amine oxidase; VAP-1, vascular adhesion protein 1; NM, *C*-naphthalen-1-yl-methylamine; DMB, 2,3-dimethoxybenzylamine; ABS, 4-aminomethyl-benzenesulfonamide; PD 0119035, 3-quinolinecarboxylic acid, 7-[3-(aminomethyl)-1-pyrrolidinyl]-6,8-difluoro-1,4-dihydro-1-(methylamino)-4-oxo; PD 0125999, 3-quinolinecarboxylic acid, 7-[3-(aminomethyl)-3-methyl-1-pyrrolidinyl]-1-cyclopropyl-6,8-difluoro-1,4-dihydro-4-oxo-, 2-hydroxypropanoate (10:11).

References

(1) Raimondi, L.; Conforti, L.; Banchelli, G.; Ignesti, G.; Pirisino, R.; Buffoni, F. Histamine lipolytic activity and semicarbazide-sensitive amine oxidase (SSAO) of rat white adipose tissue (WAT). *Biochem. Pharmacol.* **1993**, *46*, 1369−1376.
(2) Lyles, G. A. Substrate-specificity of mammalian tissue-bound semicarbazide-sensitive amine oxidase. *Prog. Brain Res.* **1995**, *106*, 293−303.
(3) Lyles, G. A.; Bertie, K. H. Properties of a semicarbazide-sensitive amine oxidase in rat articular cartilage. *Pharmacol. Toxicol.* **1998**, *60*, 33.
(4) Lizcano, J. M.; Balsa, D.; Tipton, K. F.; Unzeta, M. The oxidation of dopamine by the semicarbazide-sensitive amine oxidase (SSAO) from rat vas deferens. *Biochem. Pharmacol.* **1991**, *41*, 1107−1110.
(5) Lizcano, J. M.; Fernandez, d. A.; Lyles, G. A.; Unzeta, M. Several aspects on the amine oxidation by semicarbazide-sensitive amine oxidase (SSAO) from bovine lung. *J. Neural Transm. Suppl.* **1994**, *41*, 415−420.
(6) Smith, D. J.; Salmi, M.; Bono, P.; Hellman, J.; Leu, T.; Jalkanen, S. Cloning of vascular adhesion protein 1 reveals a novel multifunctional adhesion molecule. *J. Exp. Med.* **1998**, *188*, 17−27.
(7) Bono, P.; Salmi, M.; Smith, D. J.; Jalkanen, S. Cloning and characterization of mouse vascular adhesion protein-1 reveals a novel molecule with enzymatic activity. *J. Immunol.* **1998**, *160*, 5563−5571.
(8) Enrique-Tarancon, G.; Marti, L.; Morin, N.; Lizcano, J. M.; Unzeta, M.; Sevilla, L.; Camps, M.; Palacin, M.; Testar, X.; Carpene, C.; Zorzano, A. Role of semicarbazide-sensitive amine oxidase on glucose transport and GLUT4 recruitment to the cell surface in adipose cells. *J. Biol. Chem.* **1998**, *273*, 8025−8032.
(9) Morris, N. J.; Ducret, A.; Aebersold, R.; Ross, S. A.; Keller, S. R.; Lienhard, G. E. Membrane amine oxidase cloning and identification as a major protein in the adipocyte plasma membrane. *J. Biol. Chem.* **1997**, *272*, 9388−9392.
(10) Enrique-Tarancon, G.; Castan, I.; Morin, N.; Marti, L.; Abella, A.; Camps, M.; Casamitjana, R.; Palacin, M.; Testar, X.; Degerman, E.; Carpene, C.; Zorzano, A. Substrates of semicarbazide-sensitive amine oxidase co-operate with vanadate to stimulate tyrosine phosphorylation of insulin-receptor-substrate proteins, phosphoinositide 3-kinase activity and GLUT4 translocation in adipose cells. *Biochem. J.* **2000**, *350* (Part 1), 171−180.
(11) Marti, L.; Morin, N.; Enrique-Tarancon, G.; Prevot, D.; Lafontan, M.; Testar, X.; Zorzano, A.; Carpene, C. Tyramine and vanadate synergistically stimulate glucose transport in rat adipocytes by amine oxidase-dependent generation of hydrogen peroxide. *J. Pharmacol. Exp. Ther.* **1998**, *285*, 342−349.
(12) Morin, N.; Lizcano, J. M.; Fontana, E.; Marti, L.; Smih, F.; Rouet, P.; Prevot, D.; Zorzano, A.; Unzeta, M.; Carpene, C. Semicarbazide-sensitive amine oxidase substrates stimulate glucose transport and inhibit lipolysis in human adipocytes. *J. Pharmacol. Exp. Ther.* **2001**, *297*, 563−572.
(13) Morin, N.; Visentin, V.; Calise, D.; Marti, L.; Zorzano, A.; Testar, X.; Valet, P.; Fischer, Y.; Carpene, C. Tyramine stimulates glucose uptake in insulin-sensitive tissues in vitro and in vivo via its oxidation by amine oxidases. *J. Pharmacol. Exp. Ther.* **2002**, *303*, 1238−1247.
(14) Fontana, E.; Boucher, J.; Marti, L.; Lizcano, J. M.; Testar, X.; Zorzano, A.; Carpene, C. Amine oxidase substrates mimic several of the insulin effects on adipocyte differentiation in 3T3 F442A cells. *Biochem. J.* **2001**, *356*, 769−777.
(15) Abella, A.; Marti, L.; Camps, M.; Claret, M.; Fernandez-Alvarez, J.; Gomis, R.; Guma, A.; Viguerie, N.; Carpene, C.; Palacin, M.; Testar, X.; Zorzano, A. Semicarbazide-sensitive amine oxidase/vascular adhesion protein-1 activity exerts an antidiabetic action in Goto-Kakizaki rats. *Diabetes* **2003**, *52*, 1004−1013.
(16) Marti, L.; Abella, A.; Carpene, C.; Palacin, M.; Testar, X.; Zorzano, A. Combined treatment with benzylamine and low dosages of vanadate enhances glucose tolerance and reduces hyperglycemia in streptozotocin-induced diabetic rats. *Diabetes* **2001**, *50*, 2061−2068.

(17) Laskowski, R. A. Surfnet—A Program for Visualizing Molecular-Surfaces, Cavities, and Intermolecular Interactions. *J. Mol. Graphics* **1995**, *13*, 323-&.
(18) Gelpi, J. L.; Kalko, S. G.; Barril, X.; Cirera, J.; de, L. C., X.; Luque, F. J.; Orozco, M. Classical molecular interaction potentials: improved setup procedure in molecular dynamics simulations of proteins. *Proteins* **2001**, *45*, 428—437.
(19) Milne, G. W. A.; Miller, J. A. The NCI Drug Information System. 1. System Overview. *J. Chem. Inf. Comput. Sci.* **1986**, *26*, 154—159.
(20) Precious, E.; Lyles, G. A. Properties of a semicarbazide-sensitive amine oxidase in human umbilical artery. *J. Pharm. Pharmacol.* **1988**, *40*, 627—633.
(21) Precious, E.; Gunn, C. E.; Lyles, G. A. Deamination of methylamine by semicarbazide-sensitive amine oxidase in human umbilical artery and rat aorta. *Biochem. Pharmacol.* **1988**, *37*, 707—713.
(22) Lyles, G. A.; Chalmers, J. The metabolism of aminoacetone to methylglyoxal by semicarbazide-sensitive amine oxidase in human umbilical artery. *Biochem. Pharmacol.* **1992**, *43*, 1409—1414.
(23) Buffoni, F. Semicarbazide-sensitive amine oxidases: some biochemical properties and general considerations. *Prog. Brain Res.* **1995**, *106*, 323—331.
(24) Bradford, M. M. A rapid and sensitive method for the quantitation of microgram quantities of protein utilizing the principle of protein-dye binding. *Anal. Biochem.* **1976**, *72*, 248—254.
(25) Fowler, C. J.; Tipton, K. F. Concentration dependence of the oxidation of tyramine by the two forms of rat liver mitochondrial monoamine oxidase. *Biochem. Pharmacol.* **1981**, *30*, 3329—3332.
(26) Holt, A.; Sharman, D. F.; Baker, G. B.; Palcic, M. M. A continuous spectrophotometric assay for monoamine oxidase and related enzymes in tissue homogenates. *Anal. Biochem.* **1997**, *244*, 384—392.
(27) Sali, A.; Blundell, T. L. Comparative protein modelling by satisfaction of spatial restraints. *J. Mol. Biol.* **1993**, *234*, 779—815.
(28) Li, R.; Klinman, J. P.; Mathews, F. S. Copper amine oxidase from Hansenula polymorpha: the crystal structure determined at 2.4 A resolution reveals the active conformation. *Structure* **1998**, *6*, 293—307.
(29) Wilmot, C. M.; Murray, J. M.; Alton, G.; Parsons, M. R.; Convery, M. A.; Blakeley, V.; Corner, A. S.; Palcic, M. M.; Knowles, P. F.; McPherson, M. J.; Phillips, S. E. Catalytic mechanism of the quinoenzyme amine oxidase from *Escherichia coli*: exploring the reductive half-reaction. *Biochemistry* **1997**, *36*, 1608—1620.
(30) Parsons, M. R.; Convery, M. A.; Wilmot, C. M.; Yadav, K. D.; Blakeley, V.; Corner, A. S.; Phillips, S. E.; McPherson, M. J.; Knowles, P. F. Crystal structure of a quinoenzyme: copper amine oxidase of Escherichia coli at 2 A resolution. *Structure* **1995**, *3*, 1171—1184.
(31) Murzin, A. G.; Brenner, S. E.; Hubbard, T.; Chothia, C. SCOP: a structural classification of proteins database for the investigation of sequences and structures. *J. Mol. Biol.* **1995**, *247*, 536—540.
(32) Bateman, A.; Birney, E.; Durbin, R.; Eddy, S. R.; Howe, K. L.; Sonnhammer, E. L. The Pfam protein families database. *Nucleic Acids Res.* **2000**, *28*, 263—266.
(33) Mizuguchi, K.; Deane, C. M.; Blundell, T. L.; Overington, J. P. HOMSTRAD: a database of protein structure alignments for homologous families. *Protein Sci.* **1998**, *7*, 2469—2471.
(34) Thompson, J. D.; Higgins, D. G.; Gibson, T. J. CLUSTAL W: improving the sensitivity of progressive multiple sequence alignment through sequence weighting, position-specific gap penalties and weight matrix choice. *Nucleic Acids Res.* **1994**, *22*, 4673—4680.
(35) Sippl, M. J. Recognition of errors in three-dimensional structures of proteins. *Proteins* **1993**, *17*, 355—362.
(36) Melo, F. Feytmans, E. Assessing protein structures with a non-local atomic interaction energy. *J. Mol. Biol.* **1998**, *277*, 1141—1152.
(37) Cornell, W. D.; Cieplak, P.; Bayly, C. I.; Gould, I. R.; Merz, K. M.; Ferguson, D. M.; Spellmeyer, D. C.; Fox, T.; Caldwell, J. W.; Kollman, P. A. A Second Generation Force Field for the Simulation of Proteins, Nucleic Acids, and Organic Molecules. *J. Am. Chem. Soc.* **1995**, *117*, 5179—5197.
(38) Ewing, T. J.; Makino, S.; Skillman, A. G.; Kuntz, I. D. DOCK 4.0: search strategies for automated molecular docking of flexible molecule databases. *J. Comput. Aided Mol. Des.* **2001**, *15*, 411—428.

JM0499211